Journal of Physics: Conference Series **530** (2014) 012024 doi:10.1088/1742-6596/530/1/012024

Study on Flow behind Backward-Facing Step in a Narrow Channel

V Uruba[1]
Institute of Thermomechanics AS CR, v.v.i., Praha, Czech Republic

E-mail: uruba@it.cas.cz

Abstract. Both statistics and dynamics of the flow-field behind a backward-facing step in a narrow channel is studied experimentally using time-resolved PIV technique. The channel width is 4 step heights, Reynolds number based on the step height was about 35 thousands. Secondary flow effect is detected clearly in the region behind the step resulting in strong 3D flow structure just behind the step. The low-frequency quasi-periodical structures appearing in the region behind the step and in the region of the flow reattachment close to the channel bottom are studied using the Oscillation Pattern Decomposition (OPD) technique. Strouhal numbers of those phenomena are very low, order of 0.01. Typical time-mean structures as well as dynamical structures are to be presented.

1. Introduction

The backward-facing step flow has been established as a benchmark configuration for separated flow studies in fluid mechanics.

The flow over a backward-facing step is a very simple as for its geometry but the flow structure is extremely complex both in space and time. The flow over the backward facing step is considered to be 2D in sense of statistical characteristics as a rule, meaning that the ratio of the step height and channel width is very high, say more than 20. Then the flow-field in the middle third channel width is pretty 2D, with constant statistical characteristics along the span. Detailed study of the flow in a narrow channel, when the ration of channel width over step height is lower than 10 is very limited within public resources. The flow-field structure model in the recirculation region behind a step in narrow channel was suggested in [5]. The flow visualization on the channel bottom just behind the step showed a kidney-shaped region, suggesting existence of recirculation vortices impinging perpendicularly to the bottom – see figure 1. Here the channel bottom is shown with result of the surface visualization using painting, published in [10]. Flow direction is from left in x direction, step edge position is $x = 0$ .The red lines correspond to vanishing streamwise mean velocity component in the measuring plane (more details see section 3.1).

The case has been studied in our lab in more details. The first publications [6,8] cover the mean flow structure, those results have been summarized in [3]. Then, the dynamical behavior of the flow-field has been studied. Information on secondary structures dynamics in prismatic channel of rectangular cross-section is in [9]. Then some studies on flow in channel with backward facing step

[1] IT ASCR, Dolejskova 5, 182 00 Praha 8, Czech Republic.

have been carried out. Analysis of velocity field dynamical behavior in a few planes perpendicular to the mean flow has been presented in [4].

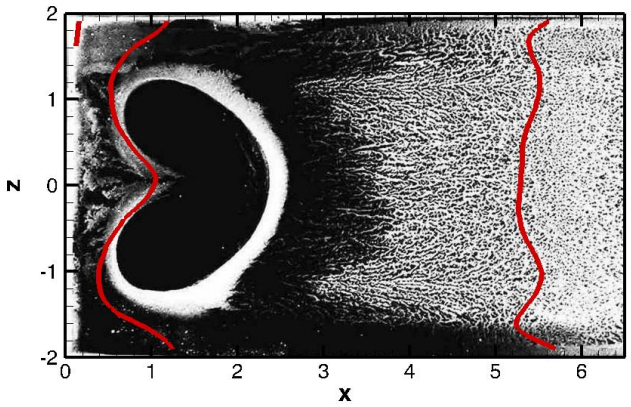

Figure 1. Surface visualization on the channel bottom.

2. Experimental Setup and Used Methods

Experimental setup and methods are to be introduced first.

2.1. Experimental Setup

The existing blow-down facility has been used for the experiments. The wind tunnel has rectangular cross-section with filled corners within the contraction (to suppress corner vortices), honeycomb and a system of damping screens followed by contraction with contraction ratio 16. The area of the test section input is 0.25 m in height and 0.1 m in width. The time mean velocity departures from homogeneity in planes perpendicular to the tunnel axis are of order tenth of per cent with the exception of corners, where corner vortex starters could be detected. The channel downstream the backward facing step was 1 m in length. The step is placed close to the channel inlet.

In the channel inlet the boundary layer thickness on the walls in the step position was about 3 mm, the step height was $h = 25$ mm. Velocity in the inlet on the step was $U_e = 20$ m/s and natural turbulence level was about 0.1 % in the working section input. The Reynolds number defined using the step height was 34 400. All presented dimensions are related to the step height and velocities to the inlet velocity U_e.

Schematic view of the experimental setup and measurement areas is given in figure 2.

The Cartesian coordinate system is defined, x is the streamwise direction, y is spanwise perpendicular to the channel bottom and z is spanwise direction parallel to the step edge. All coordinates values are non-dimensioned using the step height. The system origin was chosen on the step edge.

Two measuring domains are defined. The first 2D domain is the *measuring plane* placed behind the step oriented parallel to the channel bottom in the distance of about 1 mm above it ($y = -0.96$). It is used mainly for studying the flow dynamics behind the step and in the reattachment region.

The second 3D domain is the *measuring cuboid* covering one half of the volume behind the step. The cuboid is filled by 20 measuring planes and mean flow characteristics are interpolated to the 3D domain. This is used only for representation of time-mean data. The remaining half of the mean-flow-field is supposed to be symmetrical.

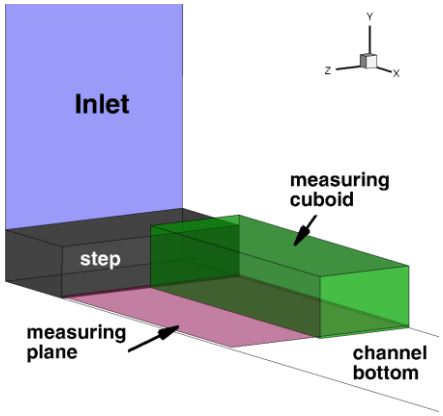

Figure 2. Experimental setup and measuring areas.

Inlet section is shown in blue, measuring cuboid in green, measuring plane in red and the step is grey.

2.2. Measuring Technique

The time-resolved PIV method was used for the experiments. The measuring system DANTEC consists of a double-pulse laser with cylindrical optics and CCD camera. The software Dynamics Studio 3.4 was used for velocity-fields evaluation. Laser New Wave Pegasus Nd:YLF, double head, wavelength 527 nm, maximal frequency 10 kHz, a shot energy is 10 mJ for 1 kHz (corresponding power 10 W per head). Camera Phantom V711 has maximal resolution 1280 x 800 pixels and corresponding maximal frequency 3000 double-snaps per second. The presented experiments are intended to cover low-frequency dynamics offering good statistics. Thus, for the measurements, the frequency 100 Hz and 4000 double-snaps in sequence corresponding to 40 s of record for mean evaluation was acquired. As the seeding source the SAFEX system has been used producing oil droplets of about 1 μm in size. Details are given in references [2-9].

2.3. Analysis Methods

The mean velocity field has been evaluated first to obtain the flow statistics and remove the mean flow. The dynamical behavior is characterized by the turbulent kinetic energy defined in usual way as a half of sum of individual velocity components variances. The dynamical behavior was studied using the Oscillation Pattern Decomposition (OPD) method, which is described in details in [5,7].

The OPD method evaluates the basis representing oscillating modes of the extended dynamical system, which are characterized by a single frequency and damping representing cyclostationary elementary processes involved in the phenomenon notwithstanding that hidden. The structure can be typically a wave or travelling structures propagating in space, or pulsating pattern represented by complex vector field.

Categorizing of the resulting vector field is performed with help of a classical approach presented in [1].

3. Results

The selected results of experiments are to be presented in following paragraphs.

First, statistical characteristics of the flow quantities distributions will be presented, then dynamical features of selected regions are to be shown.

3.1. Statistics

Statistical characteristics were evaluated in all inspected regions, i.e. in the 3D domain – measuring cuboid and in the 2D region – measuring plane. In all figures the kidney shape (in black) and $U = 0$

lines (in red) are shown. Please note that the kidney is located on the bottom ($y=-1$), while lines of vanishing mean streamwise velocity component are in the measuring plane ($y=-0.96$), so in the perspective view the alignment of the curves is affected.

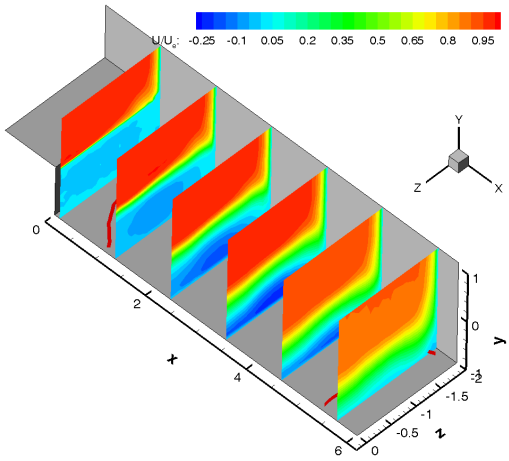

Figure 3. Streamwise velocity component distribution.

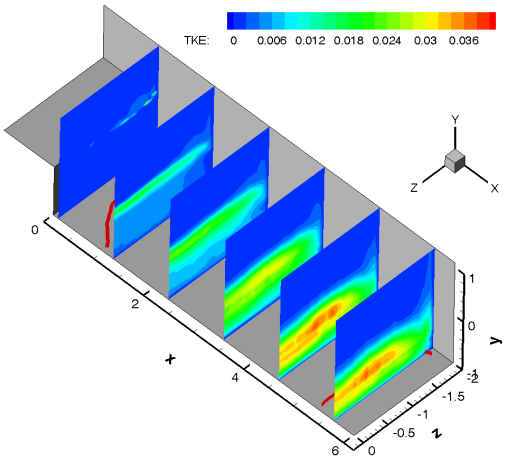

Figure 4. Kinetic energy distribution.

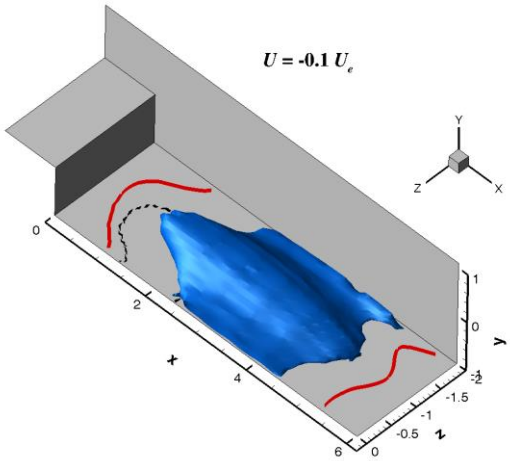

Figure 5. Iso-surface $U=-0.1U_e$.

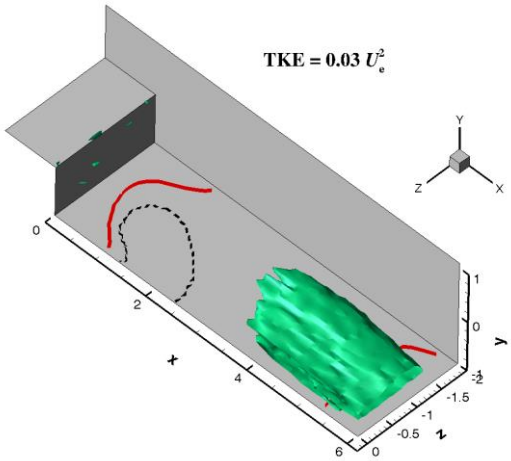

Figure 6. Iso-surface $\mathrm{TKE}=0.03U_e^2$.

In figures 3 and 4 distributions of streamwise mean velocity component U and turbulent kinetic energy are shown in 6 planes $z=const$. Both velocities and kinetic energy are non-dimensioned using the velocity in the channel inlet U_e .

Position of the recirculation region (in blue) could be recognized clearly with local maximum of back-flow velocity in position $z=-1$.

Just behind the step the kinetic energy maximum is located within the free shear layer in the step edge height ($y=0$) falling down in the streamwise direction. In the reattachment region $x=5.5$ its position is about half step bellow $y=-0.5$.

Then, the iso-surfaces of constant mean streamwise and spanwise vertical components and shown in figures 5 and 6. The back-flow region shape is clearly visible in figure 5, in figure 6 the high kinetic energy region is shown located above the reattachment region.

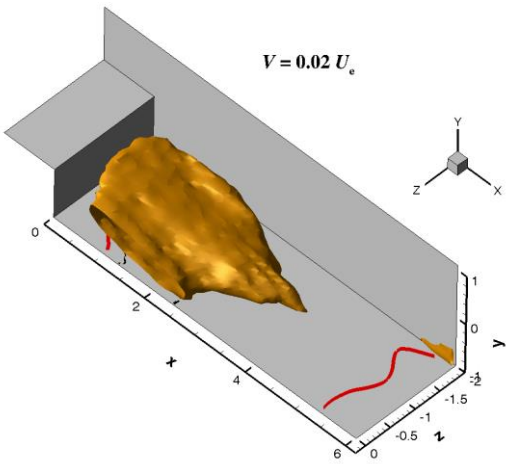

Figure 7. Iso-surface $V = 0.02U_e$.

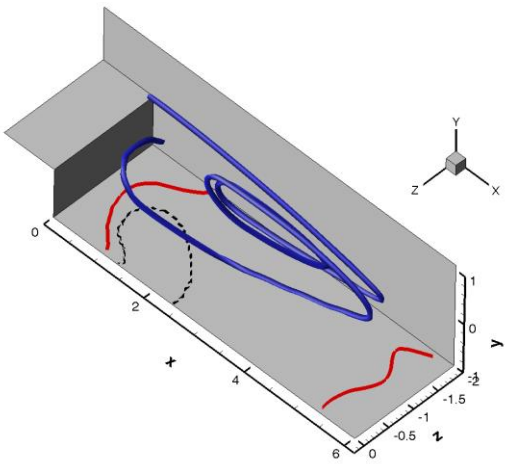

Figure 8. Vector-line of the time-mean velocity field.

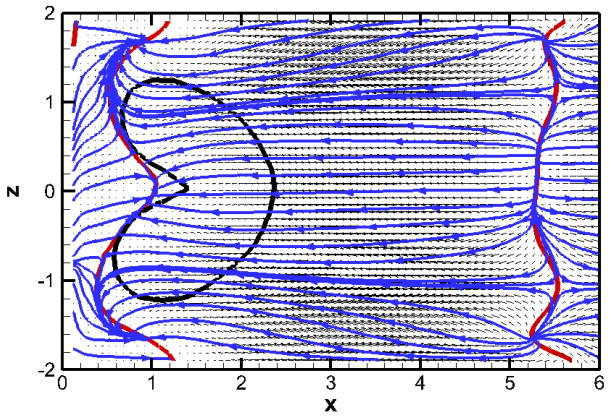

Figure 9. The mean velocity field in the measuring plane.

In the recirculation region the vertical spanwise mean velocity component seems to be of great importance. In figure 7 there is iso-surface of $V = 0.02U_e$. The spiky shape streamwise oriented is located just above the kidney pattern on the channel bottom.

Topology of the recirculation region is characterized by the vector-line of the time-mean velocity field shown in figure 8, the line originated in the channel corner just above the step.

The flow pattern in the measuring plane above the channel bottom is analyzed as well. In figure 9 the vector lines are added in blue, in red the contour of the kidney structure is given. The black lines represent the position of vanishing longitudinal mean velocity component U, dividing the area into parts with forward ($U > 0$) and backward ($U < 0$) mean flow. Note that between the black lines in the figure middle the back-flow region is located. Forward flow direction close to the step for $0 < x < 1$ is connected with appearance the tertiary vortex, while secondary vortex generates back-flow close to the bottom.

For the purpose of dynamical behaviour analysis the measuring plane has been divided into 2 parts. The first region is located just behind the step, where the kidney structure appears $x \in (0;2.5)$, the second is the flow reattachment region $x \in (4.5;6.5)$.

3.2. Dynamics of the Region just behind the Step

The region behind the step is studied first. The dominant 3 modes are those with biggest e-folding time and/or periodicity value. For the given case, the modes 1, 2 and 3 could be considered as dominant. Topology of the dominant modes is shown in Figures 10, 11 and 12. The modes topology is represented by vector fields of real and imaginary parts of the spatial mode. To visualize the structures involved (especially vortices), vector-lines (in blue) are added.

The dominant modes are all oscillating with travelling character. Topology is characterized by attracting focuses representing vortices.

For the OPD mode 1, the real and imaginary parts are in figure 10, the cores of vortices are marked by circles in red with numbers. The mode parameters, namely corresponding Strouhal number, frequency, e-folding time and periodicity was respectively: $\mathrm{Sr}_1 = 0.0094$, $f_1 = 8.18$ Hz, $\tau_{e1} = 37.7$ ms, $p_1 = 0.308$.

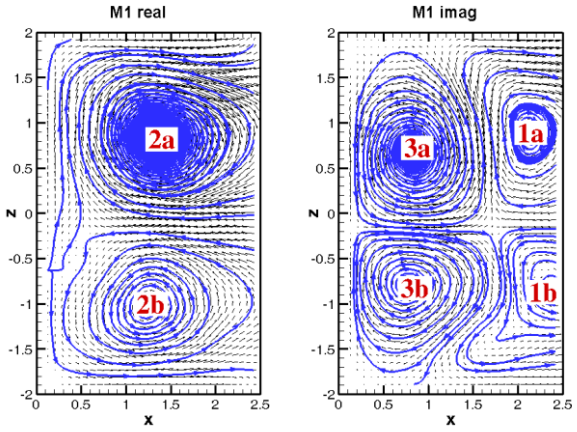

Figure 10. The OPD mode 1 in the flow behind the step.

In figure 10 a pair of contra-rotating vortices with alternative orientation travelling against the step periodically is captured. The vortices are marked “a” and “b”. The process could start by vortices in positions 1a, 1b (in the imaginary part). The vortex pair moves towards the step reaching in time corresponding to a quarter of the period position 2a, 2b (see real part). In the time half period (i.e. 61 ms) the vortices reach positions 3a, 3b, however theirs orientation is still the same. In imaginary part of figure 10 the situation of the vortices in position 3 is related to preceding vortex pair with opposite orientation. Thus, the OPD mode 1 represents the ***train of contra-rotating vortex pairs*** oriented in y direction with distance about 1.5 in z direction moving towards the step by the mean velocity of about 0.0146 of the inlet velocity U_e. The vortex pairs appear periodically in trains changing theirs orientation on the regular basis during the single mode appearance.

The OPD mode 2 is shown in figure 11. The mode relevant parameters: $\mathrm{Sr}_2 = 0.0079$, $f_2 = 6.85$ Hz, $\tau_{e2} = 24.6$ ms, $p_2 = 0.168$. The topology shows two vortices of the same orientation, 1a and 1b, moving to the position 2a and 2b, the vortex 2c appears in the same time a quarter of the period in the channel center. Then all 3 vortices of the same orientation merge into a single vortex 3 in half period time 73 ms. The last stage of the development is represented by the vortex 4 located just behind the step in the channel middle. The process is repeated periodically, however the opposite oriented vortices are involved with the shift equal to a half process period. The vortices cores (a and b) mean velocity is about 0.0122 of the U_e. Thus, the OPD mode 2 represents ***coalescence of the co-rotating vortices into a single vortex*** of the same orientation.

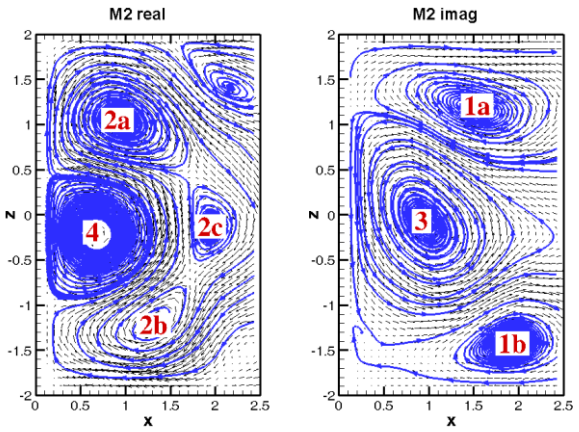

Figure 11. The OPD mode 2 in the flow behind the step.

The last dominant OPD mode 3 is shown in Figure 12. The mode relevant parameters: $\mathrm{Sr}_3 = 0.0129$, $f_3 = 11.14$ Hz $\tau_{e3} = 23.3$ ms, $p_3 = 0.259$. The mode could be interpreted as splitting of the single vortex 1 located on the channel axis into two smaller vortices 2a and 2b moving towards the step corners by mean velocity of about $0.0133\ U_e$. The next stages in a quarter period distances are 3a, 3b and finally 4a, 4b. The vortices cores are just filling the kidney-shaped area, shown in green. Thus, the OPD mode 3 represents ***splitting of the central vortex into two co-rotating vortices***, all vortices of the same orientation.

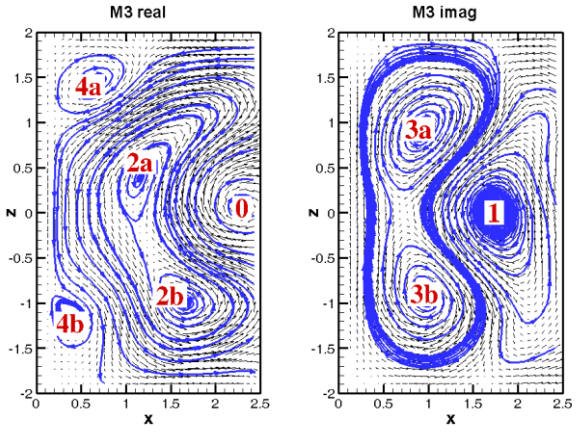

Figure 12. The OPD mode 3 in the flow behind the step.

The OPD mode 3 is the most probably directly connected with development of the kidney structure on the channel bottom, especially its downstream contour (on the right-hand side). The contour close to the step is connected with the zero U line (confirm figure 9).

3.3. Dynamics of Reattachment Region

Dynamics of the reattachment region is completely different in comparison with the region just behind the step. The typical patterns are the nodes in streamwise orientation of alternatively repealing and attracting character. A few saddle points and focuses could be recognized.

As an example the OPD mode 2 is shown in figure 13. The mode relevant parameters: $\mathrm{Sr}_2 = 0.0088$, $f_2 = 7.61$ Hz $\tau_{e3} = 15.8$ ms, $p_2 = 0.120$. This mode involves attracting nodes (red arrows) repealing nodes (green arrows) as well as a saddle point (green square). The mode dynamics could be interpreted as ***transversely moving nodes*** in *z* direction though the region.

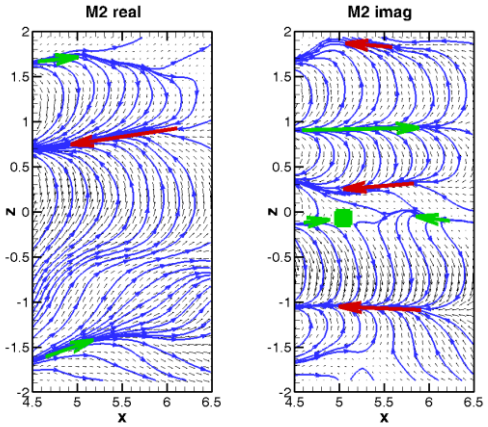

Figure 13. The OPD mode 2 in the reattachment region.

However, the OPD modes in the reattachment region are typically decaying with a small periodicity value.

4. Conclusions

The flow-field statistics and low-frequency dynamics of the flow behind the backward-facing step in narrow channel have been analyzed in the presented paper.

The results suggest presence of several families of vortical structures with particular dynamics involving contra-rotating vortex pairs train, vortex splitting and coalescence and travelling nodes.

5. References

[1] Helman J, Hesselink L 1989 *IEEE Computer* **22**, 8 27
[2] Uruba V 2014 *EPJ Web of Conferences* **67** 02120
[3] Uruba V 2013 *Colloquium FLUID DYNAMICS 2013* 35 http://www.it.cas.cz/cs/kolokvium-dynamika-tekutin-2013?q=en/node/5039
[4] Uruba V 2013 *EPJ Web of Conferences* **45** UNSP 01108
[5] Uruba V 2012 *EPJ Web of Conferences* **25** 01095
[6] Uruba V 2012 *Colloquium Fluid Dynamics 2012* 33 http://www.it.cas.cz/cs/kolokvium-dynamika-tekutin-2012?q=en/node/4886
[7] Uruba V 2012 *XX Fluid Mechanics Conference XX. Gliwice* 152
[8] Uruba V, Jonáš P 2012 *Proceedings in Applied Mathematics and Mechanics* **12** 1 501
[9] Uruba V, Hladík O, Jonáš P 2011 *Journal of Physics Conference Series* **318** 062021
[10] Uruba V, Jonáš P, Mazur O 2007 *International Journal of Heat and Fluid Flow* **28** 4 665

Acknowledgements

This work was supported by the Grant Agency of the Czech Republic, project No. P101/10/1230.